Pamukkale Univ Muh Bilim Derg, 31(7), 1150-1163, 2025

Pamukkale Üniversitesi Mühendislik Bilimleri Dergisi

Pamukkale University Journal of Engineering Sciences

Optimization of the design parameters of pressurized compound cylinders for equivalent stress and total cost

Basınçlı bileşik silindirlerde tasarım parametrelerinin eşdeğer gerilme ve toplam maliyet açısından optimizasyonu

Mevlüt Aydın[1*], *Abdullah Çakan*[1], *Mevlüt Türköz*[1]

[1]Department of Mechanical Engineering, Faculty of Engineering and Natural Sciences, Konya Technical University, Konya, Türkiye.
maydin@ktun.edu.tr, acakan@ktun.edu.tr, mturkoz@ktun.edu.tr

Received/Geliş Tarihi: 18.02.2025 Revision/Düzeltme Tarihi: 17.05.2025 doi: 10.5505/pajes.2025.88107
Accepted/Kabul Tarihi: 22.05.2025 Research Article/Araştırma Makalesi

Abstract

The optimal design of compound cylinders is crucial due to their high-pressure load-bearing requirements and significant manufacturing costs. This study focuses on optimizing the design parameters of compound cylinders to achieve minimal equivalent stress and production costs. To this end, a weighted multi-objective Grey Wolf Optimization (GWO) algorithm was employed. Furthermore, the influence of design parameters on shrinkage pressure and the equivalent stresses of the inner and outer cylinders was analyzed using detailed statistical methods. As a result of the multi-objective optimization, two reference designs were considered for comparison: one prioritizing minimum stress and the other minimizing manufacturing cost. Both the design parameter levels and weight ratios were systematically optimized. Using the optimal weight ratios and the GWO method, the maximum equivalent stress in the inner cylinder increased by 20%, while the total cost was reduced by a factor of 2.75. Consequently, a design with sufficient structural reliability was achieved, significantly lowering the manufacturing costs of compound cylinders.

Keywords: Compound cylinder, Design parameter, Grey wolf algorithm, Multi-Objective-Optimization, Total cost.

Öz

Bileşik silindirlerin tasarımı, yüksek basınç taşıma gereksinimleri ve önemli üretim maliyetleri nedeniyle büyük önem taşımaktadır. Bu çalışma, bileşik silindirlerin tasarım parametrelerini, minimum eşdeğer gerilme ve üretim maliyeti elde edecek şekilde optimize etmeyi amaçlamaktadır. Bu doğrultuda, ağırlıklı çok amaçlı Bozkurt Optimizasyonu (BO) algoritması kullanılmıştır. Ayrıca, tasarım parametrelerinin arayüzey basıncı ve iç-dış silindirlerin eşdeğer gerilmeleri üzerindeki etkisi ayrıntılı istatistiksel yöntemlerle analiz edilmiştir. Çok amaçlı optimizasyon sonucunda, karşılaştırma amacıyla iki referans tasarım ele alınmıştır: biri minimum gerilmeye öncelik veren, diğeri ise üretim maliyetini en aza indiren tasarımdır. Hem tasarım parametre seviyeleri hem de ağırlık oranları sistematik olarak optimize edilmiştir. Optimum ağırlık oranları ve BO yöntemi kullanılarak, iç silindirdeki maksimum eşdeğer gerilme %20 artarken, toplam maliyet 2.75 kat azaltılmıştır. Böylece, yeterli yapısal güvenilirliğe sahip bir tasarım elde edilerek, bileşik silindirlerin üretim maliyeti önemli ölçüde düşürülmüştür.

Anahtar kelimeler: Bileşik silindir, Tasarım parametreleri, Bozkurt algoritması, Çok amaçlı optimizasyon, Toplam maliyet.

1 Introduction

Thick-walled cylinders (TWC) are defined as cylinders with a wall thickness of at least ten times the inside radius [1]. TWCs are one of the widely used metal structures in many engineering fields [2]. TWCs are used in the hydraulic, chemical, machinery manufacturing, petroleum, military, and nuclear power plant industries. There are many applications, such as high-pressure reactor vessels, rocket engines, process plants, air compressor units, hydraulic tanks, extrusion containers, barrels, and gas storage tanks [3]. TWCs generally work under high pressures, and both hoop and radial stresses occur in TWCs. These stresses are not evenly distributed throughout the wall thickness of the cylinder [4]. The resulting stresses are not only due to internal pressure on the cylinders. As a result of their shrink fit, a significant amount of tension occurs. The manufacturing method of the cylinder, finishing method, notch effect, and radii (closed-end cylinders) affect the stresses in TWCs and reduce their fatigue life. However, the dimensions of the cylinders are the most critical factor in the occurrence of these stresses. In engineering applications, compound cylinders are used instead of thickening the walls to reduce stresses in TWCs working under high pressures. Compound cylinders consist of two or more TWCs assembled by shrink-fitting them to each other. Shrink fit is a non-permanent assembly process performed without the use of any fasteners. The shrink-fit process is done as follows: the outer cylinder is heated and then expanded, and the inner cylinder is pressed into the hub of the outer cylinder. The primary purpose of the shrink-fit process is to both assemble and create a shrinkage pressure at the interface [4]. Shrinkage pressure generates compressive stresses on the outer surface of the inner cylinder. It has been proved analytically and numerically in many studies that this effect of the shrinkage pressure reduces the maximum equivalent stresses, especially when working under internal pressure. As a result of the stress state generated by the shrink fit, a metal structure that resists higher pressures is manufactured by using less material than the total material used in a single cylinder [5]. There are methods to reduce stress levels in order to increase the fatigue life of the cylinders. Using shrink-fitted compound cylinders is one of them. A schematic and real illustration of the shrink-fit process is shown in Figure 1.

*Corresponding author/Yazışılan Yazar

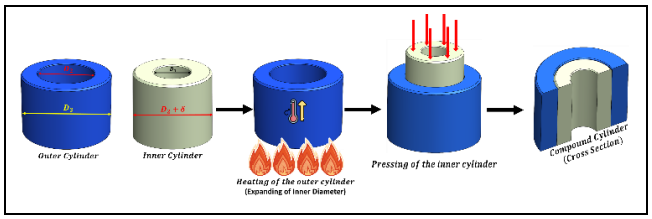

(a)

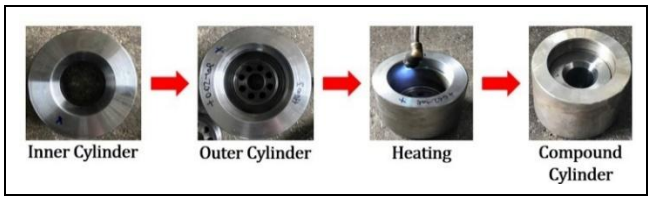

(b)

Figure 1. Illustration of the shrink-fit process. (a): Schematic, (b): Real.

Firstly, the shrinkage allowance (δ) is determined, and the cylinders are manufactured by adding this tolerance to the outer diameter of the inner cylinder. Then, the outer cylinder is heated and is waiting for expansion. Expansion varies according to the type of material and the maximum temperatures that can be reached. After expansion, the inner cylinder is centered into the outer cylinder and pressed to the hub. The cylinders are then allowed to cool. During cooling, the puckering of the outer cylinder is prevented by the inner cylinder, thus creating shrinkage pressure. The shrinkage pressure acts as an external pressure applied to the outer surface of the inner cylinder. High tensile stresses in the cylinders operating under high internal pressure may cause the part to fatigue after a while. In compound cylinders, the shrinkage pressure creates localized residual compressive stresses and increases the fatigue life [6]. Therefore, the calculation of the stresses in TWCs is very important for safe design and determination of the amount of material to be used. Radial and hoop stresses and shrinkage pressures of compound and unlayered TWCs under internal pressure were first analytically calculated by French engineer G. Lame in 1833 [7]. These stresses are used for simple geometry cylinders. Finite element methods (FEM) have been developed for more complex structures [5]. In the literature, there are many analytical and numerical calculations of the stress of compound cylinders and the changes in the fatigue life of the cylinders with the shrink fit process [3],[5],[6],[8].

One of the critical areas of use of compound cylinders is "pressure intensifiers," which sheds light on this study. Ultra-high pressures are used in industry for hydroforming, water jet cutting, sealing, blast resistance, and fatigue tests. In addition, ultra-high pressures are also used in autofrettage, industrial cleaning, and high-pressure pasteurization processes, which increase the pressure-bearing capacity of structures. Ultra-high pressures are achieved using pressure intensifiers. By using pressure intensifiers, ultra-high pressures of 200-600 MPa are obtained. In pressure intensifiers, as shown in Figure 2, the low-pressure chamber is a standard hydraulic cylinder and operates with standard hydraulic pressures such as 25 MPa. The pressure of the liquid-filled into the high-pressure chamber is increased by the area ratio [3]. At ultra-high pressures, damage in the cylinders can be dangerous and costly.

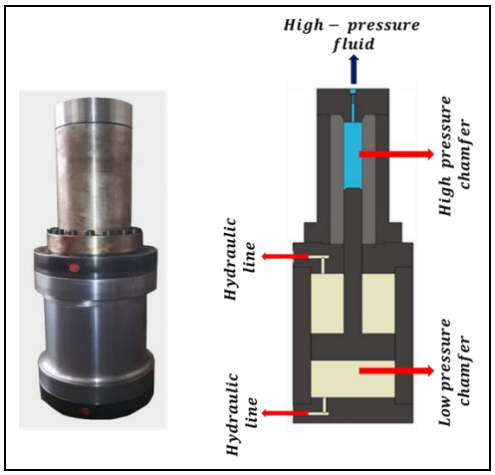

(a) (b)

Figure 2. Illustration of the pressure intensifier with 350 MPa working pressure [9]. (a): Real, (b): Schematic.

For this reason, TWCs, which are subjected to cyclic high stresses in pressure intensifiers, are generally manufactured in multiple layers and from materials with high yield and fatigue strength. In addition, it is also important to determine the dimensions that can be used safely in the design of hydraulic cylinders.

The pressure intensifier in Figure 2 operates as a single-acting hydraulic cylinder and can generate a maximum pressure of 350 MPa pressure. At such high pressures, high radial and hoop stresses occur in both the inner and outer cylinders of the high-pressure chamber. In the high-pressure chamber, pressure intensifiers operating under ultra-high pressures may cause fatigue damage. The hypothesis of this study was based on the fatigue damage and fracture of the pressure intensifier (shown above) while operating under a pressure of 350 MPa. The pressure intensifier that caused fatigue damage is shown in Figure 3.

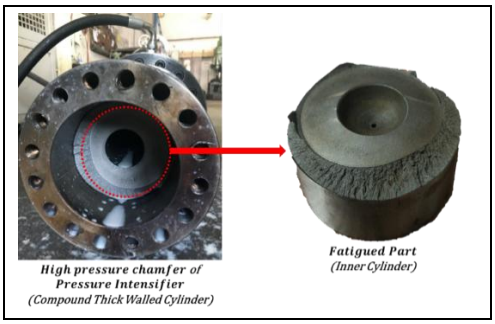

Figure 3. Fatigue damage in the Pressure intensifier [9].

In metal constructions operating under high pressures, the factor of safety should be kept high. Furthermore, the design should be analytically and numerically examined experimentally. In the industry, the wall thickness of the inner cylinder is generally increased to ensure the safety of such constructions. However, some studies in the literature show that thickening the inner cylinder is not the most critical change that can lead to stress reduction and decreased fatigue life [3]. The dimensions of the outer cylinder and the minimal shrinkage allowance are of high importance for the stresses in the cylinders.

Paredes et al. have studied shrink-fitted fasteners in an elastic region. They used the Lame formula to analyze the average contact stress in the hole walls and verified the analytical results by finite element analysis and experimental methods [10]. Benuzzi and Donzella examined the forces applied in the shrink-fitting of a railway axle and wheel with a complex structure using analytical and numerical studies [11]. It is concluded that SEA results are better than analytical results for complex components. Öztürk analytically and numerically evaluated the shrinkage pressure occurring at different interference tolerances of thick-walled compound cylinders with steel-steel and steel-aluminum materials [5]. The stresses that occurred in the shrink-fitting process were calculated by FEA along the wall and compared with analytical values. As a result of the comparisons, it was stated that FEMs successfully estimated the shrinkage pressures in the compound cylinders. In addition, it has been stated that FEAs are more reliable than analytical methods in determining the stresses of shrink-fitted parts with complex geometry. Özel et al. analyzed the stress and deformation for different hub-shaft connections by FEA to determine the shrinkage allowance [12]. The stresses on the outer surface of the inner cylinder were analytically calculated and verified by Lame equations. Similar to other studies in the literature, it is stated that Finite Element results are more valuable than analytical results in the calculations of shrink-fitted specimens with complex geometry. As a result of the studies, it was stated that the end regions of the cylinders are more unsafe, and higher stresses occur than in the center regions. Aydin et al. have investigated the effect of shrinkage pressure on the fatigue life of cylinders in shrink-fitted compound cylinders [6]. As a result of the FEAs, fatigue life increased as the shrinkage allowance increased. Under the same conditions, the life of the single-layer cylinder was 5586 cycles, while the life of the optimum compound cylinder increased by 99% to 9530 cycles. In the study by Aydın and Türköz, it was found by numerical analyses that the weight can be reduced by up to 36% compared to a single-layer structure in compound cylinder designs formed with different material pairs [13]. Aydin et al. calculated the maximum equivalent stresses occurring in the compound cylinders used in pressure intensifiers analytically and numerically [3]. They then conducted a validation study. They concluded that the most influential parameter in the inner cylinder at 350 MPa internal pressure is the shrinkage allowance. They also proved that the inner cylinder wall thickness does not contribute to the maximum stress and fatigue life of the material. Akay and Rıdvanoğulları researched the optimum turning process parameters for the shrink fit in the train wheel [14]. The surface roughness must be in the range of 0.8-3.2 micrometers in order for this shrink fit to be adequately performed. In order to achieve these levels, they optimized the cutting depth, feed, and cutting girl parameters. Campos and Hall have simplified Lame's equations [15]. Simplified formulas and classical Lame equations were compared with SEA results. The simplified equations were found to agree with both results. In addition, it has been found that the radial stress does not depend on the thickness in thin-walled shrink-fit processes. Wang et al. proposed a new theoretical model that predicts nonuniform stress distributions in shrink-fitted constructions [16]. Experiments and analytical analysis have validated the theoretical model. In the study, contact length and shrinkage ratio in the shrink fit process were also investigated as effect parameters. Stress distributions of different material pairs (Ni36CrTiAl - 50Ni-50Fe, AISI 1045 - AISI 1045) at full contact conditions were analyzed. As a result, the theoretical model has been shown to have high accuracy in estimating the stress distribution. It is stated that the same model can be used in different material pairs. Wang et al. stated that non-uniformly contacting regions will cause stress concentration, and this causes deviations in the results in Lame equations [17]. Wang et al. derived a stress formulation in a double-layer TWC operating under internal pressure [18]. They also used the bi-modulus of the material while deriving this formulation. Zhu et al. produced a composite elastoplastic solution for a double-layer or multi-layer cylinder using the ratio of tensile strength σ_t to compressive strength σ_c. In addition to the importance of estimating the stresses occurring in compound TWCs, it is also very important to make the optimum geometric design according to these stresses [19]. Designers must present ideas that reduce stresses while reducing material and manufacturing costs. This problem raises an optimization problem.

The originality of this study is to optimize the compound cylinder used in pressure intensifiers for total equivalent stress, total weight, and manufacturing cost using the grey wolf algorithm. The detailed statistical analysis and multi-objective weighted optimization for total equivalent stress and total cost of compound cylinders were performed for the first time in the literature. In this context, it is aimed at designing both lower cost and constructions with lower stresses at ultra-high pressures. The performance criteria in this study are, respectively, the interface pressure, the maximum stress occurring in the inner cylinder, the maximum stress occurring in the outer cylinder, and the total cost. The maximum stress values of the outer cylinder were constrained, and the parameters were optimized by determining the optimal weights of the total cost, as well as the maximum stress that occurred in the inner cylinder. After that, constrained and weighted optimization performed using the optimal weight ratios. The results of this study will shed light on the industrial organizations that design compound cylinders and academic studies on the subject.

2 Material and method

In this study, the compound high-pressure chambers of pressure intensifiers used to achieve ultra-high pressures such as 450 MPa will be optimized in terms of total equivalent stress and total cost. In this context, the effects of the inner radius of the inner cylinder (R_1) the thickness of the inner cylinder (T_1), the thickness of the outer cylinder (T_2), and the shrinkage allowance (δ) on the shrinkage pressure, the maximum equivalent stresses in the inner cylinder and the total cost (material and manufacturing) were investigated. The optimum parameter levels were obtained for two different scenarios. The parameters were given schematically in Figure 4. In Figure 4, the inner radius of the inner cylinder is indicated by R_1, outer radius of the inner cylinder by R_2, outer radius of the outer cylinder by R_3, the wall thickness of the inner cylinder by T_1, and the wall thickness of the outer cylinder by T_2. The outer radius of the inner cylinder (which is also the inner radius of the outer cylinder) is given by $R_1 + T_1$, while the outer radius of the entire assembly is $R_1 + T_1 + T_2$. The symbol δ represents the shrink fit allowance (interference) between the inner and outer cylinders.

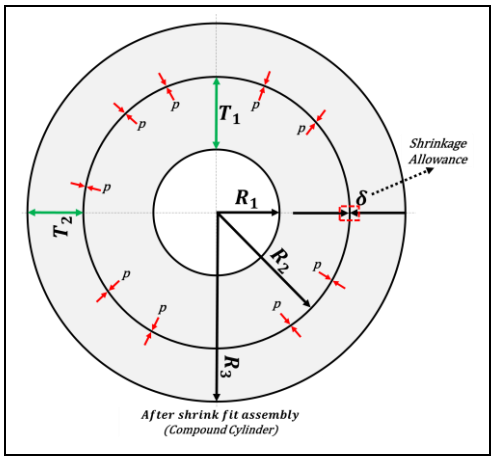

Figure 4. Schematic representation of shrink fit assembly and shrinkage allowance.

2.1 Shrinkage pressure and stress calculation in compound cylinder

High stresses occur in TWCs operating under ultra-high pressure. Properly dimensioned construction is crucial for operating under high stresses without damage. In compound TWCs, the shrinkage pressure generates a pre-stress in the compression direction on the inner cylinder surfaces. The compressive pre-stress in the inner cylinder reduces the tensile stress resulting from the internal pressure. In fact, the compressive stresses on the inner surface increase the fatigue strength of the structure by preventing the progression of micro-cracks. Therefore, compound cylinders can withstand much higher stresses than single-layer cylinders of equivalent thickness. The number of layers is decided according to the intensity of the internal pressure and the resulting stresses. The assembly of compound cylinders is done by press-fitting or heating. The most widely used assembly process is the heated fitting process. To assemble the cylinders, the outer cylinder is heated, and the inner cylinder is inserted into it. In the meantime, due to the size difference, the so-called "shrinkage pressure" (p) occurs at the interface [7]. Equation 1 shows the formula of the interface pressure resulting from the shrink fit of two cylinders [20]. In the formula, E represents the modulus of elasticity of the material.

The radial (σ_r) and hoop (σ_h) stresses occur in TWCs under internal and external pressures. The stresses in the inner and outer cylinders are shown schematically in Figure 5.

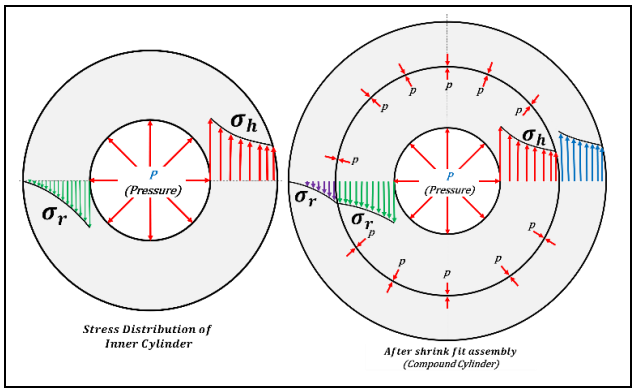

Figure 5. Stress distribution of inner and compound cylinders under inner and shrinkage pressure.

Lame equations (Equations 2 and 3) are used for the calculation of stresses [20]. In the equations, E is the modulus of elasticity, ν is the Poisson's ratio, r is a constant indicating at which radius "r" of the cylinder the stress is calculated, and C is the stress constant. C_1 and C_2 are constants that vary with internal and external pressure and are shown in Equations 4 and 5. In this equations p_i is the inner pressure, p_o is the outer pressure.

$$p = \frac{E * \delta}{R_2} * \frac{(R_2^2 - R_1^2) * (R_3^2 - R_2^2)}{2 * R_2^2 * (R_3^2 - R_1^2)} \quad (1)$$

$$\sigma_r = \frac{E}{1 - v^2} * \left[C_1 * (1 + v) - C_2 * \frac{1 - v}{r^2}\right] \quad (2)$$

$$\sigma_h = \frac{E}{1 - v^2} * \left[C_1 * (1 + v) + C_2 * \frac{1 - v}{r^2}\right] \quad (3)$$

$$C_1 = \frac{1 - v}{E} * \left[\frac{(R_1^2 * p_i) - (R_2^2 * p_o)}{(R_2^2 - R_1^2)}\right] \quad (4)$$

$$C_2 = \frac{1 - v}{E} * \left[\frac{R_1^2 * R_2^2 * (p_i - p_o)}{(R_2^2 - R_1^2)}\right] \quad (5)$$

Radial and hoop stresses calculated (in equation 6 and 7) as when C and C_2 values are substituted in Equations 2 and 3;

$$\sigma_r = \left[\frac{(R_1^2 * p_i) - (b^2 * p_o)}{(R_2^2 - R_1^2)}\right] - \left[\frac{(p_i - p_o) * R_1^2 * b^2}{r^2 * (R_2^2 - R_1^2)}\right] \quad (6)$$

$$\sigma_h = \left[\frac{(R_1^2 * p_i) - (R_2^2 * p_o)}{(R_2^2 - R_1^2)}\right] + \left[\frac{(p_i - p_o) * R_1^2 * R_2^2}{r^2 * (R_2^2 - R_1^2)}\right] \quad (7)$$

To determine the maximum equivalent stress in the cylinder, the Von-Mises equivalent stress theory was used;

$$\sigma_{eq.} = \sqrt{\sigma_r^2 - \sigma_r * \sigma_h + \sigma_h^2} \quad (8)$$

2.2 Calculation of total cost in compound cylinders

Total cost is an important factor in the manufacture of compound cylinders in pressure intensifiers. This study aims to optimize the dimensions of cylinders operating at ultra-high pressures, which are planned to be manufactured at low stresses and low costs. Hence, material and machining costs were taken into account when calculating the total cost. Compound cylinders are generally manufactured by turning hollow cylinders. In order to normalize the material cost, the cylinder materials will be considered as solid cylinders. Firstly, the volumes of the inner and outer cylinders in each experiment were calculated, and then the weights were calculated by multiplying the density of the steels (7.8 g/cm^3). The liquid volume capacity of the pressure intensifier whose TWC was designed was determined as 0.3 liters. Therefore, the internal volume of the inner cylinder was 0.3 liters (300000 mm^3). Due to the different diameter of the inner cylinder, the lengths of all cylinders were calculated as shown in Equation 10 to fix the volume capacity.

$$V_{cylinder} = \pi * R_1^2 * l_{cylinder} \quad (9)$$

$$l_{cylinder} = \frac{300{,}000}{\pi * R_1^2} \quad (10)$$

The total material cost was then found by multiplying the market value of AISI 4340 (inner cylinder) and AISI 1050 (outer

cylinder). The total weight and total cost calculation are detailed in equations 11-15, respectively. In the equations, V represents the volume, l represents the cylinder length, and m represents the mass.

$$V_{inner} = \pi * R_2^2 * l\ [mm^3] \quad (11)$$

$$V_{outer} = \pi * R_3^2 * l\ [mm^3] \quad (12)$$

$$m_{inner} = V_{inner} * 7.8x10^{-6}\ (kg) \quad (13)$$

$$m_{outer} = V_{outer} * 7.8x10^{-6}\ (kg) \quad (14)$$

$$Total\ Cost_{material} = m_{inner}(kg) * 20\left(\frac{\$}{(kg)}\right) + m_{outer}(kg) * 12(\frac{\$}{(kg)}) \quad (15)$$

For the manufacturing cost of the cylinders, the machining cost presented in literature [21]-[23] is adapted in this study. In calculation, we assumed that the tool must be replaced when one operation is finished. The total cost for the compound cylinders was calculated by summation of $Total\ Cost_{material}$ and $Total\ Cost_{manufacturing}$. The total cost for manufacturing formulated as follows:

$$Total\ Cost_{manufacturing} = C_o * T_u + C_t * \frac{T_C}{T} \quad (16)$$

where C_o is the operating cost per minute ($3\$/min$), C_t is the cutting tool cost ($10\$/piece$), T_u is the total manufacturing time, T_c is the turning time, and T is the tool life. The operation cost C_o is the combination of labor and depreciation cost. The total manufacturing time, T_u, is defined as follows:

$$T_u = T_C + \frac{T_C}{T} * T_R + T_L + T_p \quad (17)$$

where T_R is the time of replacing the used cutting tool, T_L is the presetting time, and T_P is the time for changing the parts. Since the cutting insert is replaced after each operation, the $\frac{T_C}{T}$ ratio is assumed to be 1. The operation times are considered as follows: T_R is 2 minutes, T_L is 2 minutes, and T_P is 3.5 minutes. The cutting time T_C is calculated using the Equation 18.

$$T_C = \frac{\pi * D * l}{v * f} \quad (18)$$

where D is the diameter of the cylinder, l is the length of the cylinder, v is the cutting speed and f is the feed value in (mm/rev). After calculating the machining costs for the inner and outer cylinders as presented above, the total manufacturing cost was determined by adding them. The total cost of the compound cylinders was calculated by summing the total material cost (given in Equation 15) and the total turning cost.

2.3 Study's methodology

A parametric optimization was performed for three different scenarios using a weighted objective function. Firstly, a full factorial design with 81 experiments consisting of four parameters and three levels of each parameter was created. Then, detailed statistical analyses were performed for all performance criteria, followed by determining the constraint for optimization. These constraints include the maximum equivalent stress in the outer cylinder. After determining the coefficient of the constraints, optimization was performed using the grey wolf algorithm based on weighted objective functions. Finally, three different scenarios were compared with the optimum levels obtained for all performance criteria.

Parameter levels shown in Table 1 were used to investigate the effects of the geometrical parameters in the TWC. The full factorial design (shown in Table 2) was used in this study. Although wall thickness is given as the second and third parameters, the results are given according to the radii of the cylinders. Regression and variance analyses were applied to the results, and the significance and effect levels of the parameters on the results were expressed in detail.

Table 1. Parameters and levels of this study.

Parameters	Parameter levels		
	1	2	3
Inner radius of inner cylinder (R_1) (mm)	17.5	25	32.5
Inner cylinder wall thickness (T_1) (mm)	15	30	45
Outer cylinder wall thickness (T_2) (mm)	15	30	45
One-sided shrinkage allowance (δ) (mm)	0.03	0.06	0.09

2.4 Detailed statistical analysis of performance criteria

In this study, detailed statistical analyses are performed for the output parameters of shrinkage pressure, maximum equivalent stress in the inner cylinder, maximum equivalent stress in the outer cylinder, and total cost. Firstly, variance analysis (ANOVA) was applied to the output parameters.

Table 2. Full factorial experimental plan.

Exp.	R_1 (mm)	T_1 (mm)	T_2 (mm)	δ (mm)
1	17.5	15	15	0.03
2	17.5	15	15	0.06
3	17.5	15	15	0.09
4	17.5	15	30	0.03
5	17.5	15	30	0.06
6	17.5	15	30	0.09
7	17.5	15	45	0.03
8	17.5	15	45	0.06
9	17.5	15	45	0.09
10	17.5	30	15	0.03
11	17.5	30	15	0.06
12	17.5	30	15	0.09
13	17.5	30	30	0.03

Table 2. Continued.

Exp.	R_1 (mm)	T_1 (mm)	T_2 (mm)	δ (mm)
14	17.5	30	30	0.06
15	17.5	30	30	0.09
16	17.5	30	45	0.03
17	17.5	30	45	0.06
18	17.5	30	45	0.09
19	17.5	45	15	0.03
20	17.5	45	15	0.06
21	17.5	45	15	0.09
22	17.5	45	30	0.03
23	17.5	45	30	0.06
24	17.5	45	30	0.09
25	17.5	45	45	0.03
26	17.5	45	45	0.06
27	17.5	45	45	0.09
28	25.0	15	15	0.03
29	25.0	15	15	0.06
30	25.0	15	15	0.09
31	25.0	15	30	0.03
32	25.0	15	30	0.06
33	25.0	15	30	0.09
34	25.0	15	45	0.03
35	25.0	15	45	0.06
36	25.0	15	45	0.09
37	25.0	30	15	0.03
38	25.0	30	15	0.06
39	25.0	30	15	0.09
40	25.0	30	30	0.03
41	25.0	30	30	0.06
42	25.0	30	30	0.09
43	25.0	30	45	0.03
44	25.0	30	45	0.06
45	25.0	30	45	0.09
46	25.0	45	15	0.03
47	25.0	45	15	0.06
48	25.0	45	15	0.09
49	25.0	45	30	0.03
50	25.0	45	30	0.06
51	25.0	45	30	0.09
52	25.0	45	45	0.03
53	25.0	45	45	0.06
54	25.0	45	45	0.09
55	32.5	15	15	0.03
56	32.5	15	15	0.06
57	32.5	15	15	0.09
58	32.5	15	30	0.03
59	32.5	15	30	0.06
60	32.5	15	30	0.09
61	32.5	15	45	0.03
62	32.5	15	45	0.06
63	32.5	15	45	0.09
64	32.5	30	15	0.03
65	32.5	30	15	0.06
66	32.5	30	15	0.09
67	32.5	30	30	0.03
68	32.5	30	30	0.06
69	32.5	30	30	0.09
70	32.5	30	45	0.03
71	32.5	30	45	0.06
72	32.5	30	45	0.09
73	32.5	45	15	0.03
74	32.5	45	15	0.06
75	32.5	45	15	0.09
76	32.5	45	30	0.03
77	32.5	45	30	0.06
78	32.5	45	30	0.09
79	32.5	45	45	0.03
80	32.5	45	45	0.06
81	32.5	45	45	0.09

Minitab 21 was used to obtain the ANOVA table, and the P-value and contribution ratio of the parameters on the results were interpreted. Then, the plots for the main effects were obtained and interpreted for all performance criteria. After ANOVA, regression analyses were performed. Within the scope of regression analysis, regression curve, R-square value, and histogram graph were obtained. The regression analysis results obtained for all performance criteria are also comprehensively interpreted.

2.5 Constrained and weighted Grey Wolf algorithm optimization for total equivalent stress and total cost

Today, optimization processes are frequently used in design and various engineering problems. The main reasons for this are environmentally friendly design, energy efficiency, cost reduction, weight reduction, and making designs more useful. In this study, the optimum design parameters of shrink-fitted cylinders were determined. In the optimization process, the grey wolf algorithm introduced by Mirjalilil et al. was used [24]. Grey wolf optimization has been used in the literature for both single-objective and multi-objective optimization problems for many different engineering disciplines [25]-[28]. There are four different grey wolf groups to mimic the leadership hierarchy of grey wolves used for the implementation of the grey wolf algorithm. In the leadership hierarchy shown in Figure 6, the first layer is alpha (α), representing the most robust and most capable head wolf. In the second layer, the beta (β) wolves command the other lower-level wolves and communicate with the alpha wolves.

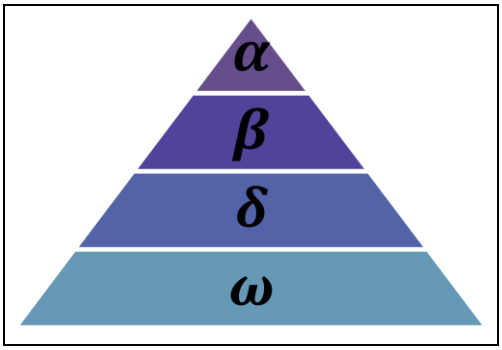

Figure 6. Hierarchy of grey wolf (dominance decreases from top down) [24].

In the optimization algorithm, they amplify the alpha's commands tra, transmit them to the lower-level wolves, and provide feedback to the alpha wolf. In the lowest layer are the omega wolves (ω), which occupy a large part of the total and are mainly responsible for stabilizing the internal relations of the population and protecting and monitoring the young wolf population. Wolves in the third stratum are categorized as delta wolves (δ), which do not belong to the other three strata and must submit to alpha and beta class wolves but dominate omega wolves [24]. MATLAB software was used to perform optimization.

Beyond their hierarchical structure, cooperative hunting is another key behavior modeled in the GWO algorithm. As outlined by Muro et al. (2011), the hunting strategy of gray wolves consists of three main stages: (i) tracking and approaching the prey, (ii) encircling and exhausting it, and (iii) launching a final coordinated attack. These stages are algorithmically mapped to exploration, encircling, and exploitation phases in GWO.

Assuming the dimension of the solution space in the GWO algorithm is d and the gray wolf population size is N, the position of the i-th gray wolf is expressed in Equation 19:

$$X_i = \{X_i^1, X_i^2, \dots\dots, X_i^d\}, \qquad i = 1,2, \dots, N \tag{19}$$

In GWO, the best, second-best, and third-best solutions are denoted as $\alpha, \beta,$ and δ, respectively, while the remaining individuals are classified as ω. The position of the α-wolf represents the estimated location of the prey, i.e., the best current solution. The encircling mechanism, which mimics the wolves' strategy to restrict prey movement, is mathematically formulated as follows:

$$\vec{D} = \left|\vec{C} * \overrightarrow{X_p}(t) - \vec{X}(t)\right| \tag{20}$$

$$\vec{X}(t+1) = \overrightarrow{X_p}(t) - \vec{A} * \vec{D} \tag{21}$$

Where t is the current iteration, $\vec{A}$ and $\vec{C}$ are the coefficient vectors, ($\overrightarrow{X_p}$) is the location vector of the prey and $\vec{X}$ is the location vector of the grey wolf. $\vec{A}$ and $\vec{C}$ vectors are calculated in Equation 22 and 23, respectively:

$$\vec{A} = 2 * \vec{a} * \overrightarrow{r_1} - \vec{a} \tag{22}$$

$$\vec{C} = 2 * \overrightarrow{r_2} \tag{23}$$

Here the components of $\vec{a}$ are linearly decremented from 2 to 0 over the iterations, and r_1, r_2 are random vectors in (0, 1) [24].

In nature, gray wolves locate and encircle their prey under the leadership of the α-wolf, with assistance from the β- and δ-wolves. In the context of optimization, the exact location of the global optimum is unknown; thus, the top three solutions-α, β, and δ-serve as guides to approximate its position. The remaining wolves, including the ω group, update their positions, accordingly, enabling the population to converge toward the optimal solution. This leadership-based hierarchy ensures that the top solutions are preserved while others adjust based on their influence [24]. This behavior is mathematically expressed by the following equations (Equations 24-30), and the overall flow of the GWO algorithm is illustrated in Figure 7.

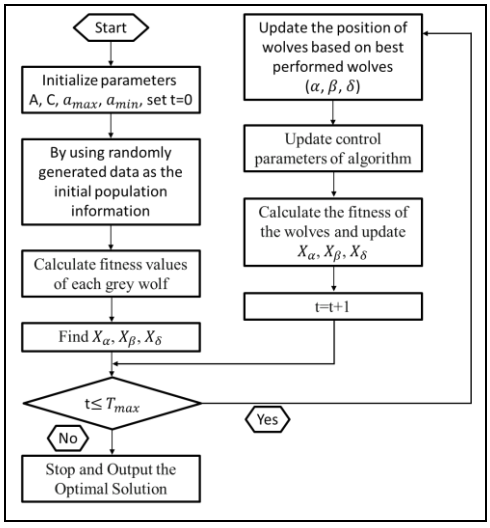

Figure 7. Flow chart of GWO algorithm [29].

$$D_\alpha = |C_1 - X_\alpha(t) - X(t)| \quad (24)$$

$$D_\beta = |C_2 - X_\beta(t) - X(t)| \quad (25)$$

$$D_\delta = |C_3 - X_\delta(t) - X(t)| \quad (26)$$

$$X_1 = X_\alpha - A_1 * D_\alpha \quad (27)$$

$$X_2 = X_\beta - A_2 * D_\beta \quad (28)$$

$$X_3 = X_\delta - A_3 * D_\delta \quad (29)$$

$$X(t+1) = \frac{X_1 + X_2 + X_3}{3} \quad (30)$$

3 Results and discussion

In this study, the shrinkage pressure, maximum equivalent stresses, and total cost, shown in Figure 8, were calculated analytically. Based on the analytical results, detailed statistical analyses were performed, and multi-objective weighted optimization was performed using the grey wolf algorithm. Details of the statistical results and the optimization process's results according to each performance criterion are described below.

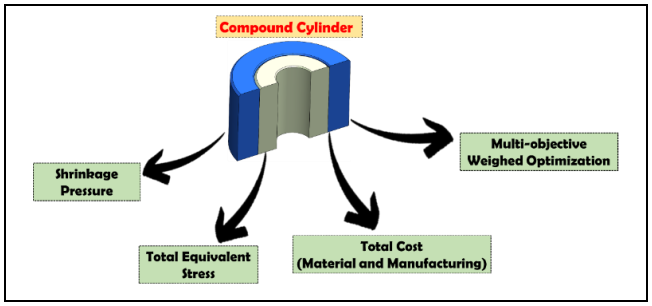

Figure 8. Output parameters and optimization of this study.

3.1 Shrinkage pressure

The shrinkage pressures of 81 different compound cylinders working under 350 MPa ultra-high internal pressure are given in Table 3. The highest shrinkage pressure was obtained at 175 MPa in the 9th design. The lowest shrinkage pressure was obtained as 11.1 MPa in the 73th design. In order to determine the effects of design variables on the shrinkage pressure variance analysis (ANOVA) were performed. To interpret the results of the ANOVA, $P-value$ and contribution ratios are usually evaluated, respectively. The $P-value$ is known as a measure of significance. A small P-value (typically less than 0.05) indicates a statistically significant difference between the means of the groups. The contribution ratio measures the proportion of the total variation in the response variable explained by a given independent variable. A high contribution ratio indicates that the independent parameter has a strong influence on the output, while a low contribution rate indicates a weak influence. The ANOVA table for the shrinkage pressure results is given in Table 4. The $P-value$ of all input parameters in the table is less than 0.05. This result shows that the input parameters have significant effects on the shrinkage pressures. The parameter with the highest contribution to the shrinkage pressure was shrinkage allowance with a rate of 47.09%. The findings of this study agree with an earlier study [5], which also showed the importance of the shrinkage allowance on the von-mises stress of the inner and outer cylinder.

Table 3. Shrinkage pressure results.

Exp.	p (MPa)	Exp.	p (MPa)	Exp.	p (MPa)
1	41.3	29	55.6	57	59.8
2	82.7	30	83.4	58	26.1
3	124.0	31	36.2	59	52.2
4	53.2	32	72.3	60	78.3
5	106.4	33	108.5	61	28.9
6	159.6	34	39.9	62	57.8
7	58.3	35	79.9	63	86.8
8	116.7	36	119.8	64	15.2
9	175.0	37	19.5	65	30.5
10	25.6	38	38.9	66	45.7
11	51.3	39	58.4	67	22.3
12	76.9	40	28.2	68	44.5
13	36.8	41	56.5	69	66.8
14	73.6	42	84.7	70	26.2
15	110.4	43	33.0	71	52.3
16	42.7	44	66.0	72	78.5
17	85.5	45	99.0	73	11.1
18	128.2	46	13.5	74	22.2
19	16.7	47	27.0	75	33.4
20	33.4	48	40.5	76	17.3
21	50.1	49	20.8	77	34.6
22	25.6	50	41.7	78	51.9
23	51.1	51	62.5	79	21.1
24	76.7	52	25.3	80	42.2
25	30.8	53	50.6	81	63.3
26	61.7	54	76.0		
27	92.5	55	19.9		
28	27.8	56	39.9		

Table 4. The ANOVA table for the shrinkage pressure results.

Source	F-value	P-value	Cont.%	Remarks
R_1 (mm)	539.5	<0.0001	15.1	Significant
T_1	581.7	<0.0001	16.2	Significant
T_2	357.8	<0.0001	10.0	Significant
Shrinkage allowance	1681.4	<0.0001	47.1	Significant
R_1* T_1	61.6	<0.0001	3.4	Significant
R_1* T_2	6.8	<0.0001	0.4	Significant
R_1* Shrinkage allowance	44.9	<0.0001	2.5	Significant
T_1* Shrinkage allowance	48.4	<0.0001	2.7	Significant
T_2* Shrinkage allowance	29.8	<0.0001	1.7	Significant
Error			0.7	
Total			100.0	

The shrinkage allowance tolerance levels selected in this study are relatively small, and controlling manufacturing is quite tricky. However, it is the most influential parameter on the pressure at the interface. Therefore, the shrinkage allowance needs to be set very precisely, and it should be as high as possible when manufacturing compound cylinders that operate under ultra-high internal pressures. The lowest contribution in terms of input parameters was the outer radius of the outer cylinder, with 10.0%. Interaction effects of the parameters were found to be low in the variance model. The error rate of the ANOVA analysis was calculated as 0.7%

A main effects plot is a type of graph used in statistics and data analysis to represent the relationship between input parameters and results visually. It is used to understand the effect of an input parameter on the result while other variables are held constant. The main effects plot for the shrinkage pressure is given in Figure 9.

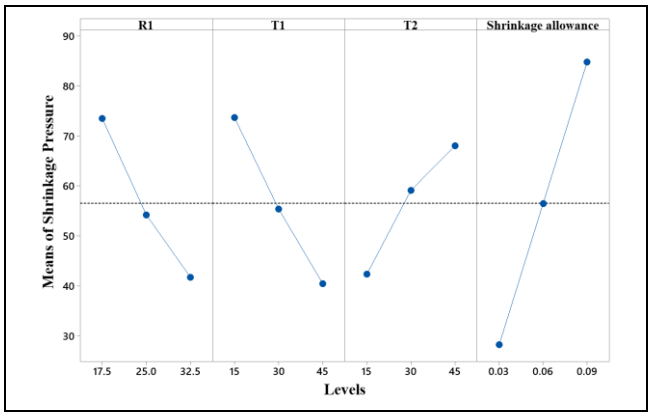

Figure 9. The main effects plot for the shrinkage pressure.

The effects of the parameters on the shrinkage pressure were linearly increasing or decreasing. While the inner radius (R_1) and thickness of the inner cylinder (T_1) are inversely proportional to the shrinkage pressure, the thickness of the outer cylinder (T_2) and shrinkage allowance (δ) are proportional to the shrinkage pressure. While the average interfacial pressure was 73 MPa at the 17.5 mm R_1, the average interfacial pressure decreased by 43% to 41 MPa when the R_1 was 32.5. The increase of T_2 caused an increase in the shrinkage pressure. However, increasing T_2 causes an increase in the amount of material, and this creates a disadvantageous situation regarding the total cost. The primary purpose of this study is to optimize by considering the total cost while doing this kind of geometric dimensioning. Considering the shrinkage allowance, the average interfacial pressure was 29 MPa with a δ of 0.03 mm, but this value increased by 193% to 85 MPa with a δ of 0.09 mm. It is desirable to increase the shrinkage pressure, but for safety reasons, the total stress in the cylinders must be calculated.

The R-squared value is a statistical measure of how well the regression curve approximates the actual data points. The R-square value ranges from 0 to 1, where 0 indicates that the model explains none of the variability around the mean of the output parameters data, and 1 indicates that the model explains all of the variability around the mean of the output parameters. A high R-squared value indicates the predictability of the outcome with a high success rate using the input parameters. R-squared adjusted is a modified version of R-squared, a statistical measure of the fit of a linear regression model. R-squared adjusted is used to compare models with more than one independent variable. R-square and R-square adjusted values are 0.983 and 0.980, respectively. It is concluded that the parameters have high predictability on the shrinkage pressure.

An interaction plot is a type of plot used to visualize the relationship between two or more input parameters and the result. It is a way to see how the effect of one parameter on the result depends on the levels of another factor. The 6 interaction graphs obtained for the shrinkage pressure are shown in Figure 10. First of all, it can be said that all interactions are proportional and as they do not coincide each other, there is not an interaction between the parameters. However, it can be observed that the effect of changing inner cylinder thickness (**T_1**) on shrinkage pressure is most pronounced when the shrinkage allowance is at its highest value. Again, it was observed that when the thickness of outer cylinder is its minimum level, there is not any effect of inner cylinder thickness.

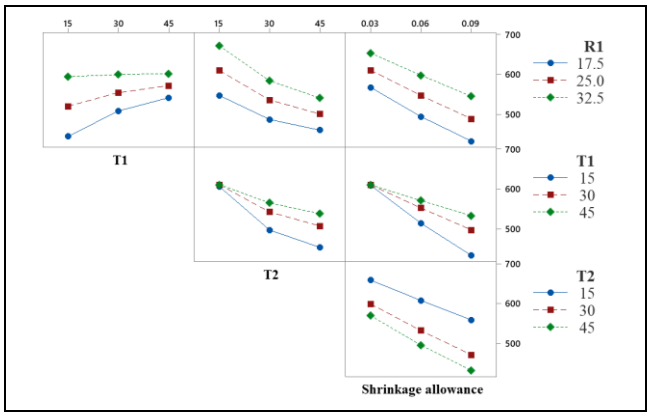

Figure 10. The interaction graphs for shrinkage pressure.

3.2 Maximum equivalent stress in the outer cylinder

The maximum equivalent stresses occurring in the outer cylinders under ultra-high internal pressure of 350 MPa are given in Table 5. The outer cylinders are generally manufactured from low-strength materials. Therefore, it is absolutely important to calculate the stresses occurring in the outer cylinder. Designing the outer cylinder as unsafe may cause sudden fatigue damage. The highest stress was obtained as 668.5MPa in the 57th design. The lowest equivalent stress was obtained as 131.9 MPa in the 25th design.

Table 5. The maximum equivalent stresses in the outer cylinder of 81 different compound cylinders.

Exp.	σ_{outer} (MPa)	Exp.	σ_{outer} (MPa)	Exp.	σ_{outer} (MPa)
1	350.1	29	525.9	57	668.5
2	489.6	30	632.9	58	426.4
3	629.1	31	370.8	59	500.4
4	320.8	32	465.5	60	574.5
5	448.6	33	560.1	61	396.3
6	576.4	34	350.9	62	465.1
7	309.4	35	440.4	63	534.0
8	432.7	36	530.0	64	293.0
9	555.9	37	245.9	65	373.6
10	205.0	38	339.4	66	454.2
11	315.8	39	432.9	67	266.7
12	426.7	40	227.6	68	340.1
13	193.2	41	314.1	69	413.5
14	297.7	42	400.6	70	253.5
15	402.2	43	218.8	71	323.3
16	188.0	44	302.0	72	393.0
17	289.6	45	385.2	73	201.0
18	391.3	46	168.9	74	270.7
19	141.9	47	247.0	75	340.4
20	230.3	48	325.0	76	187.6
21	318.7	49	159.3	77	252.7
22	135.2	50	232.9	78	317.7
23	219.4	51	306.5	79	180.2
24	303.7	52	154.2	80	242.8
25	131.9	53	225.5	81	305.3
26	214.1	54	296.7		
27	296.3	55	496.2		
28	419.0	56	582.4		

The ANOVA table for the maximum equivalent stress in the outer cylinder is given in Table 6. The P-value of all input parameters in the table is less than 0.05. These results show that changing the levels of the input parameters has statistically significant effects on the equivalent stress of the outer cylinder.

Table 6. The ANOVA table for the maximum equivalent stress in the outer cylinder.

Source	F-value	P-value	Cont.%	Remarks
R1 (mm)	805.6	<0.0001	2.1	Significant
T1	6488.6	<0.0001	61.8	Significant
T2	46.1	<0.0001	2.47	Significant
Shrinkage allowance	1090.0	<0.0001	30.9	Significant
R1* T1	19.2	<0.0001	0.1	Significant
R1* T2	23.2	<0.0001	0.2	Significant
R1* Shrinkage allowance	5.5	<0.0001	0.8	Significant
T_1* T_2	22.8	<0.0001	0.8	Significant
T1* Shrinkage allowance	136.2	<0.0001	0.4	Significant
T2* Shrinkage allowance	16.2	<0.0001	0.1	Significant
Error			0.23	
Total			100.0	

However, the thickness of the inner cylinder (T_1) was the most important parameter, with a contribution rate of 61.8%, and the effects of the other parameters were less pronounced. While the contribution rate of the δ was calculated as 30.1%, the effect of R_1 and T_2 seems nearly no effect on its stress value with a contribution rate of 2.1% and 2.4%, respectively. The main effects plot of the parameters is given in Figure 11.

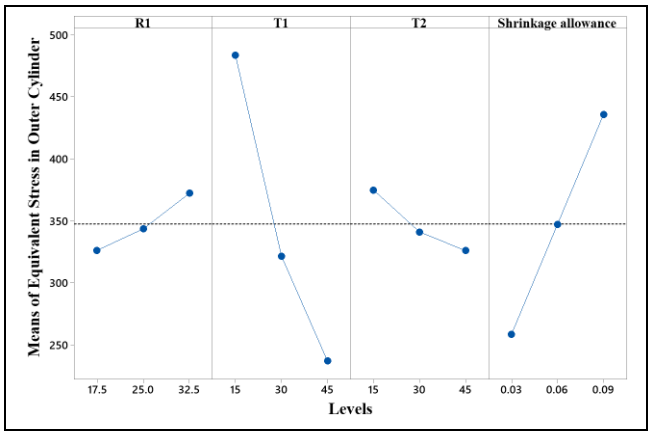

Figure 11. The main effects plot for the maximum equivalent stress in the outer cylinder.

As can be seen from the figure, an increase in the R_1 and a decrease in T_2 parameters causes a slight increase in the stress level. The stress level decreases significantly with the increase in the T_1 parameter. Again, increasing $\boldsymbol{\delta}$ caused an increase in the stress level. An interesting result is that there is no need to increase the thickness of the outer cylinder to reduce the stress level in the outer cylinder. This information is important for designing the compound cylinders as safely and economically.

The R-squared and R-squared adjusted values are 0.997 and 0.996, respectively. R-square adjusted values of 0.7 and above are accepted in engineering problems. So, it is concluded that the parameters have high predictability on the maximum equivalent stress in the outer cylinder. When the interaction plots given in Figure 12 are examined, it is seen that there is only a slight interaction between the parameters of R_1 and δ. When the level of δ was 0.03 mm changing of R_1 affected the stress level but when it is 0.09, changing of R_1 did not affect the stress of outer cylinder.

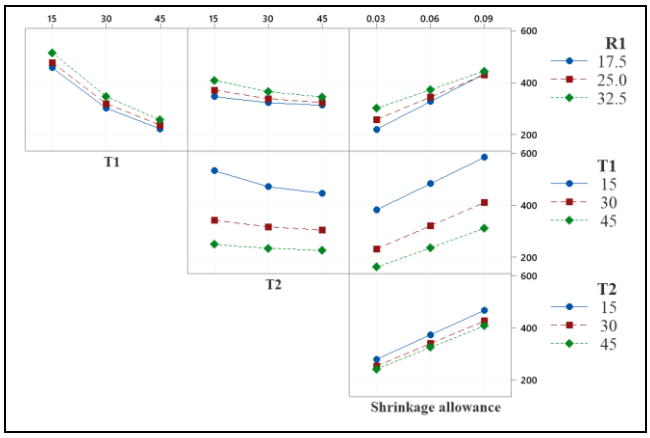

Figure 12. The interaction graphs for maximum equivalent stress of outer cylinders.

3.3 Maximum equivalent stress in the inner cylinder

The maximum equivalent stresses occurring in the inner cylinder of 81 different compound cylinders when internal pressure was 350 MPa are given in Table 7.

Table 7. The maximum equivalent stresses in the inner cylinder of 81 different compound cylinders.

Exp.	σ_{inner} (MPa)	Total Cost ($)	Exp.	σ_{inner} (MPa)	Total Cost ($)	Exp.	σ_{inner} (MPa)	Total Cost ($)
1	600.6	534	29	606.0	395	57	636.4	330
2	503.5	534	30	528.9	395	58	651.1	386
3	416.5	534	31	592.1	479	59	566.2	386
4	530.0	686	32	493.9	479	60	486.2	386
5	416.0	686	33	406.8	479	61	597.4	454
6	331.9	686	34	551.1	584	62	506.7	454
7	500.5	878	35	447.5	584	63	424.6	454
8	382.9	878	36	362.1	584	64	701.5	506
9	311.0	878	37	652.9	654	65	664.1	506
10	606.4	986	38	609.9	654	66	627.2	506
11	555.8	986	39	567.9	654	67	639.0	574
12	507.1	986	40	602.0	759	68	586.0	574
13	565.5	1179	41	541.7	759	69	534.8	574
14	495.7	1179	42	484.4	759	70	605.1	654
15	431.5	534	43	574.9	883	71	544.3	654
16	544.3	534	44	506.1	883	72	486.3	654
17	465.5	534	45	442.3	883	73	669.2	727
18	395.7	686	46	637.1	989	74	645.2	727
19	607.4	686	47	610.0	989	75	621.6	727
20	576.3	686	48	583.4	989	76	631.0	806
21	545.8	878	49	605.2	1114	77	594.6	806
22	580.9	878	50	564.4	1114	78	558.9	806
23	534.3	878	51	524.7	1114	79	607.8	898
24	489.7	986	52	586.1	1259	80	564.0	898
25	565.3	986	53	537.3	1259	81	521.5	654
26	510.1	986	54	490.5	1259			
27	458.0	1179	55	771.5	330			
28	686.5	1179	56	703.2	330			

The highest stress was obtained in experiment 55 as 771.5 MPa. The lowest equivalent stress was obtained in the 9th design as 311 MPa. However, since the outer cylinder stress exceeded the allowable stress in the 9th design, the lowest equivalent stress was 395 MPa in the 18th design. The ANOVA table is given in Table 8. The P-value of all input parameters in the table is less than 0.05. This result shows that all input design parameters have significant effects on the equivalent stress in the inner cylinder. Except for the thickness of the inner cylinder (T_1), all design parameters exhibit similar effects on the stress level. The shrinkage allowance (δ) contributes the most with a ratio of 32.7%, while the thickness of the outer cylinder (T_2) and the inner radius of the inner cylinder (R_1) have effects of 27.4% and 22.3%, respectively.

Table 8. The ANOVA table for the maximum equivalent stress in the inner cylinder.

Source	F-value	P-value	Cont.%	Remarks
R1 (mm)	1199.8	<0.0001	22.3	Significant
T1	333.3	<0.0001	6.2	Significant
T2	1476.6	<0.0001	27.4	Significant
Shrinkage allowance	1757.2	<0.0001	32.7	Significant
R1* T1	81.5	<0.0001	3.0	Significant
R1* T2	19.5	<0.0001	0.7	Significant
R1* Shrinkage allowance	7.2	<0.0001	0.3	Significant
T_1* T_2	70.7	<0.0001	2.6	Significant
T1* Shrinkage allowance	97.6	<0.0001	3.6	Significant
T2* Shrinkage allowance	15.5	<0.0001	0.5	Significant
Error			0.4	
Total			100.0	

These results also verified the results of a previous study conducted according to Taguchi L9 orthogonal design [3]. The parameters have high predictability on the maximum equivalent stress in the inner cylinder. Because R-square and R-square adjusted values are 0.976 and 0.972, respectively. The main effects plot for the maximum equivalent stress in the inner cylinder is given in Figure 13.

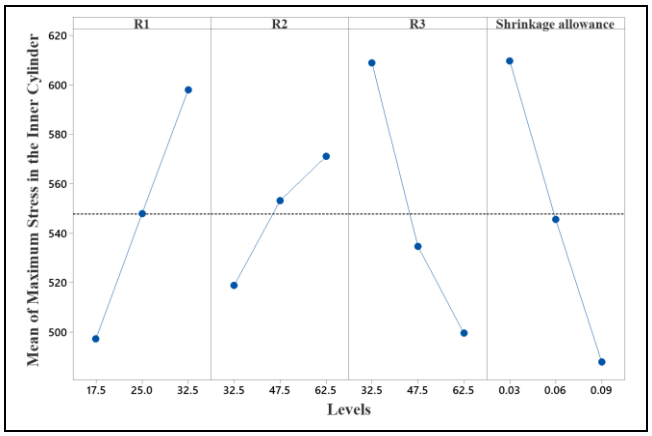

Figure 13. The main effects plot for the maximum equivalent stress in the inner cylinder.

While increasing R_1 caused a significant increase in the stress value, conversely, increasing T_2 and δ reduced the stress level considerably. Despite its minimal effect, interestingly, an increase in T_1 caused a higher stress level. That is because as the inner cylinder wall thickness increases, the outer cylinder wall thickness decreases and therefore the compressive stress in the inner cylinder decreases. The reduction in equivalent stress observed in the compound cylinder is consistent with the findings of Aydın et al. who demonstrated that outer layers significantly lower the tensile stresses in the inner cylinder under internal pressure [3],. When interaction plots given in Figure 14 were examined, there is an interaction between T_1 and δ. T_1 does not have any effect when δ has 0.03 mm. In the design of compound cylinders, T_1 is generally taken at maximum values in order to make a safe design. However, the results showed that it should be taken with minimum dimensions. The inner cylinders are generally manufactured from high-strength and overcasting materials. Therefore, designing compound cylinders to have minimum T_1 will also provide a more economical solution.

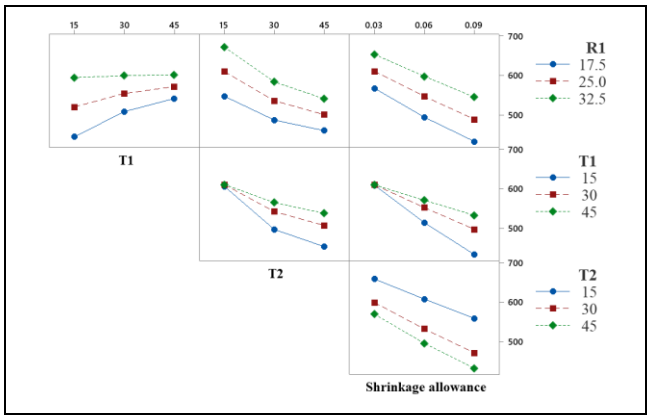

Figure 14. The interaction graphs for maximum equivalent stress of inner cylinders.

Again, for a more economical design, instead of increasing T_2, it is recommended to select the δ value at higher levels so as not to cause yield in the outer cylinder. The smaller R_1 reduces the stress of inner cylinder but for a given volume capacity, the length of the cylinders should be increased as the radius decreases. Therefore, an optimization is required for the economical design of the compound cylinders.

3.4 Determination of optimum parameter levels using the constrained Grey Wolf Algorithm

Before the optimization process, reference parameter levels were determined for comparison. The reference parameter levels are the parameter levels that give the minimum stress in the inner cylinder (18th design in Table 7) and the lowest total cost (58th design in Table 7). The designs with an equivalent stress in the outer cylinder above the safety yield strength (430 MPa) are excluded from the full factorial design table. These reference values are called Ref_1 and Ref_2. The parameter levels of Ref_1 and Ref_2 and the results obtained at these two reference levels are shown in Table 9.

Table 9. Parameter levels, maximum equivalent stresses, and total cost of reference compound cylinders.

	R_1 (mm)	T_1 (mm)	T_2 (mm)	δ (mm)	σ_{inner} (MPa)	σ_{outer} (MPa)	Total Cost ($)
Ref_1	17.5	30	45	0.09	395	391	1413
Ref_2	32.5	15	30	0.03	651	426	386

The objective functions for the equivalent stress in the inner cylinder and total cost are given by eq. 31 and 32 are given respectively

$$\begin{aligned} &Equivalent\ stress\ of\ inner\ cylinder\ (MPa) \\ &= 564.7 + 14.14 * R_1 + 2.995 * T_1 \\ &- 7.779 * T_2 - 4194 * \delta - 0.0059 \\ &* R_1^2 - 0.0366 * T_1^2 + 0.0867 * T_2^2 \\ &+ 3615 * \delta^2 - 0.1986 * R_1 * T_1 \\ &- 0.0978 * R_1 * T_2 + 29.33 * R_1 * \delta \\ &+ 0.08812 * T_1 * T_2 + 54.36 * T_1 * \delta \\ &- 21.11 * T_2 * \delta \end{aligned} \quad (31)$$

$$\begin{aligned} Total\ Cost\ (\$) &= 921 - 90.36 * R_1 + 48.99 * T_1 + 17.88 \\ &* T_2 + 2.272 * R_1^2 + 0.2032 * T_1^2 \\ &+ 0.0544 * T_2^2 - 1.6019 * R_1 * T_1 \\ &- 0.6196 * R_1 * T_2 + 0.1088 * T_1 * T_2 \end{aligned} \quad (32)$$

In this study, the optimization process was conducted by applying weighting to the mathematical models of output

parameters. This weighting approach facilitates the simultaneous evaluation of multiple objectives within the optimization process. By assigning a specific level of importance to each objective, weighting enables the integration of all objectives into a single objective function. Mathematically, the total weighted objective function can be represented as:

$$F_{total} = w_1 * f_1(x) + w_2 * f_2(x) \quad (33)$$

Where w_i is the weight assigned to the objective function f_i and these weights reflect the degree of priority or importance between the objectives. In the present study, two distinct performance criteria weighted to execute the optimization process.

The weight ratios for the two objective functions total cost and equivalent stress of inner cylinder were optimized for finding the best weight ratio. The optimization of the weight ratios was done as follows.

Optimum parameter levels were obtained with a total of nine different weight ratios starting from 90% (σ)-10% ($Total\ Cost$) up to 10% (σ)-90% ($Total\ Cost$). σ and Total Cost (T.C.) are the objective functions for the equivalent stresses in the inner cylinder and total cost of compound cylinders, respectively. Equivalent stresses in the inner cylinder and the total costs were calculated using nine different weighed optimization as shown in Table 10.

Table 10. The parameter levels and results obtained for all weight ratios.

Exp. No	Weight Ratios	R_1	T_1	T_2	δ	σ_{inner} (MPa)	Total Cost
1	0.9*σ + 0.1*T.C.	17.50	15	50.39	0.062	369	970
2	0.8*σ + 0.2*T.C.	30.43	23.25	58.24	0.090	423	664
3	0.7*σ + 0.3*T.C.	26.07	15	46.16	0.055	467	535
4	0.6*σ + 0.4*T.C.	26.63	15	39.85	0.051	500	473
5	0.5*σ + 0.5*T.C.	26.22	15	30.70	0.045	547	415
6	0.4*σ + 0.6*T.C.	26.10	15	23.62	0.040	600	373
7	0.3*σ + 0.7*T.C.	25.83	15	16.67	0.034	668	336
8	0.2*σ + 0.8*T.C.	25.28	15	11.74	0.030	727	314
9	0.1*σ + 0.9*T.C.	24.67	15	10.53	0.03	736	313

Since the two performance criteria do not have same units, the equivalent cylinder of the inner cylinder and total cost was normalized according to Eq. 34. Hence the equivalent stress and normalized cost results obtained for nine different weight ratios were calculated as shown in Table 11.

$$|x|_{normalized} = \frac{x - x_{min}}{x_{max} - x_{min}} \quad (34)$$

After the normalization process the results of the equivalent stresses and total costs were shown in the same graph as in Figure 15. The optimum weight ratios were determined as the intersection point of two-line graphs (Stress and Total cost). As a result, the optimum weight ratios were calculated as 67% for equivalent stress and 33% for the total cost.

The optimization was done again by using the optimum weight ratio. The optimization results with optimum weight ratio were given in Table 12.

Table 11. The equivalent stress and normalized cost results.

Weight Ratios	σ_{inner} (normalized)	Total Cost $_{normalised}$
0.9*σ + 0.1*T.C.	0.000	1.000
0.8*σ + 0.2*T.C.	0.147	0.534
0.7*σ + 0.3*T.C.	0.267	0.338
0.6*σ + 0.4*T.C.	0.357	0.244
0.5*σ + 0.5*T.C.	0.485	0.155
0.4*σ + 0.6*T.C.	0.629	0.091
0.3*σ + 0.7*T.C.	0.815	0.035
0.2*σ + 0.8*T.C.	0.975	0.002
0.1*σ + 0.9*T.C.	1.000	0.000

Table 12. Optimization results (comparison with reference compound cylinders).

	σ_{inner}(MPa)	Total Cost ($)
Ref_1	395	1413
Ref_2	651	386
Optimum Levels (Opt_Weighted)	477	514

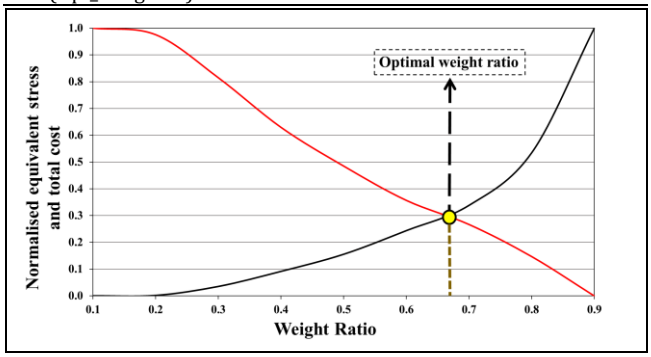

Figure 15. The graphical representation of the results for the ten weight ratios.

The optimum values of $\mathbf{R_1}$, $\mathbf{T_1}$, $\mathbf{T_2}$ and $\boldsymbol{\delta}$ were 26.42 mm, 15 mm, 44.66 mm and 0.054 mm, respectively. The results were compared with the parameter levels which gives minimum equivalent stress in the inner cylinder (Ref_1) and the parameter levels which gives minimum total cost of compound cylinder (Ref_2). The optimization led to a 20% increase in maximum equivalent stress; however, this value remains within safe design limits and is accompanied by a remarkable 2.75-fold reduction in total cost. This configuration offers a well-balanced and highly efficient solution. This result shows that it is possible to achieve significant cost reduction by allowing some increase in stress. Compared to the Ref_2, there is a significant reduction in equivalent stress level of 26.7%. As a result, thanks to multi-objective optimization, both an economical and safe design has been achieved.

4 Conclusions

The design of compound thick-walled cylinders is very important to obtain safety and economical solutions. Cylinders designed with high safety coefficients are manufactured at very high costs. Therefore, optimum design parameter levels should be calculated. The main objective of this study is firstly determine the effect of geometrical design parameters of compound cylinders on their stress values. Secondly determine the optimum design parameter levels of compound thick-walled cylinders. As a result of the study, the optimum dimensions of compound thick-walled cylinders with low stress levels and economical cost were determined. The outputs of the study are summarized below:

1) The most effective parameter of the shrinkage pressure was the shrinkage allowance (δ). Very small changes in shrinkage allowance cause significant changes in shrinkage pressure and stress levels,
2) The parameter with the highest contribution to the equivalent stress in the outer cylinder was the thickness of the inner cylinder (T_1) and there is nearly no effect of the thickness of the outer cylinder on its stress. Therefore, there is no need to increase the thickness of the outer cylinder to reduce the stress level of its,
3) Except for the thickness of the inner cylinder (T_1), almost all parameters affect the maximum stresses of the inner cylinder to almost the same degree. Therefore, the T_1 value should be chosen as low as possible to achieve a more economical design,
4) The smaller inner cylinder radius (R_1) reduces the stress of inner cylinder but for a given volume capacity, the length of the cylinders should be increased as the radius decreases. Therefore, an optimization is required for the economical design of the compound cylinders,
5) For a more economical design, instead of increasing thickness of the outer cylinder (T_2), it is recommended to select the shrinkage allowance (δ) value at higher levels so as not to cause yield in the outer cylinder,
6) As a result of multi-objective weighted optimization to get the optimal solution in terms of safety and cost, the optimum weight ratios were calculated as 67% for equivalent stress and 33% for the total cost,
7) As a result of the optimization, the maximum equivalent stress in the inner cylinder increased by 20% (395 MPa to 477 MPa) while the total cost decreased by 2.7 times (1413$ to 514$),
8) Using the optimum design parameters instead of the parameters that give the minimum cost, there is a significant reduction in the equivalent stress of the inner cylinder by 26.7% (651 to 477 MPa).

5 Authors contribution statements

Stress calculations, design, and statistical analysis were carried out by Mevlüt Aydın and Mevlüt Türköz. Abdullah Çakan carried out optimization procedures and algorithms.

6 Ethics committee approval and conflict of interest statement

"There is no need to obtain an ethics committee approval in the manuscript".

"There is no conflict of interest with any person/institution in the manuscript".

7 References

[1] Phalguna BN. "Stress and failure analysis of thick walled cylinder with oblique hole". *Internatioanl Journal of Engineering Research and Technology*, 6(8), 36-45, 2017.
[2] Yuanhan W. "Torsion of a thick-walled cylinder with an external crack: boundary collocation method". *Theoretical and applied fracture mechanics*, 14(3), 267-273,1990.
[3] Aydın M, Türköz M, Yapan YF. "Ultra Yüksek Basınçta Çalışan Kalın Cidarlı Silindirlerin Tasarımına Etki Eden Parametrelerin Sayısal ve Analitik Olarak Araştırılması". *Konya Journal of Engineering Sciences*, 10(2), 412-424, 2022.
[4] Booker JD, Truman CE, Wittig S, Mohammed Z. "A comparison of shrink-fit holding torque using probabilistic, micromechanical and experimental approaches". *Proceedings of the Institution of Mechanical Engineers, Part B: Journal of Engineering Manufacture*, 218(2),175-187, 2004.
[5] Ozturk F. "Finite-element modelling of two-disc shrink fit assembly and an evaluation of material pairs of discs". *Proceedings of the Institution of Mechanical Engineers, Part C: Journal of Mechanical Engineering Science*, 225(2),263-273, 2011.
[6] Aydin M, Yapan, YF, Turkoz, M. "Investigation on Effect of Shrinkage Allowance to the Fatigue Life of Compound Cylinders Operating at High Pressure". *International Conference on Engineering Technologies*, 370-374, 2020.
[7] Ugural AC, Saul KF. Advanced mechanics of materials and applied elasticity. Pearson Education, 2011.
[8] Zhang Y, McClain B, Fang XD. "Design of interference fits via finite element method". *International Journal of Mechanical Sciences*, 42(9),1835-1850, 2000.
[9] Aydın M, Türköz M. "A study on the effect of the roller burnishing process on the axial fatigue performance and surface integrity of AISI 4340 steel". *Journal of the Brazilian Society of Mechanical Sciences and Engineering*, 44(6), 224, 2022.
[10] Paredes M, Naoufel N, Marc S. "Study of an interference fit fastener assembly by finite element modelling, analysis and experiment". *International Journal on Interactive Design and Manufacturing*, 6,171-177, 2012.
[11] Benuzzi D, Donzella G. "Prediction of the press-fit curve in the assembly of a railway axle and wheel". *Proceedings of the Institution of Mechanical Engineers, Part F: Journal of Rail and Rapid Transit*, 218, 51-65, 2004.
[12] Özel A, Temiz Ş, Aydin MD, Şen S. "Stress analysis of shrink-fitted joints for various fit forms via finite element method". *Materials & design*, 26(4), 281-289, 2005
[13] Aydın M, Türköz M. "Effect of shrink fit process on total equivalent stress and total amounf of material". *International Conference on Engineering Technologies*, 405-408, 2021.
[14] Akay ME, Ridvanogullari A. "Optimisation of machining parameters of train wheel for shrink-fit application by considering surface roughness and chip morphology parameters". *Engineering Science and Technology, an International Journal*, 23(5), 1194-1207, 2020.
[15] Campos UA, David EH. "Simplified Lamé's equations to determine contact pressure and hoop stress in thin-walled press-fits". *Thin-Walled Structures*, 138, 199-207, 2019.
[16] Wang X, Lou Z, Wang X, Hao X, Wang Y. "Prediction of stress distribution in press-fit process of interference fit with a new theoretical model". *Proceedings of the Institution of Mechanical Engineers, Part C: Journal of Mechanical Engineering Science*, 233(8), 2834-2846, 2019.
[17] Wang X, Lou Z, Wang X, Xu C. "A new analytical method for press-fit curve prediction of interference fitting parts". *Journal of Materials Processing Technology*, 250, 16-24, 2017.

[18] Wang S, Zhu Q, Zhao JH, Yue XP, Jiang YJ. "Elastoplastic assessment of limiting internal pressure in thick-walled cylinders with different tension-compressive response". *Strength of Materials*, 51, 508-519, 2019.
[19] Zhu Q, Wang S, Zhang DF, Jiang YJ, Yue X. "Elastoplastic analysis of ultimate bearing capacity for multilayered thick-walled cylinders under internal pressure". *Strength of Materials*, 52, 521-531,2020.
[20] Harvey JF. Theory and design of pressure vessels. 2nd ed. New York, USA, VNR Company, 1991.
[21] Groover MP. *Fundamentals of Modern Manufacturing: Materials, Processes, and Systems*. 4th ed. Danvers, USA, *John Wiley & Sons*, 2010.
[22] Stephenson DA, Agapiou JS. Metal cutting theory and practice. 3rd ed. Florida, USA, CRC press, 2018.
[23] Chung C, Wang PC, Chinomona B. "Optimization of turning parameters based on tool wear and machining cost for various parts". *The International Journal of Advanced Manufacturing Technology*, 120(7), 5163-5174,2022.
[24] Mirjalili S, Mirjalili SM, Lewis A. "Grey wolf optimizer". *Advances in Engineering Software*, 69, 46-61, (2014).
[25] Şen MA, Kalyoncu M. "Grey wolf optimizer based tuning of a hybrid LQR-PID controller for foot trajectory control of a quadruped robot". *Gazi University Journal of Science*, 32(2), 674-684, 2019.
[26] Baş E, İhsan E. "Gri kurt optimizasyonu ve krill sürü optimizasyon algoritmasının performans analizi ve karşılaştırması". *Pamukkale Üniversitesi Mühendislik Bilimleri Dergisi,* 29(7), 711-736, 2023.
[27] Gürkan E, Güner A. "FV sistemlerde kısmi gölgeleme koşullarında maksimum güç noktası takibi için metasezgisel algoritmaların karşılaştırmalı performans analizi". *Pamukkale Üniversitesi Mühendislik Bilimleri Dergisi,* 30(7), 891-905, 2024.
[28] Beştaş MŞ, Dinler ÖB. "Kötü amaçlı android tabanlı yazılım tespitinin trend meta-sezgisel algoritmalar ile karşılaştırılmalı analizi". *Pamukkale Üniversitesi Mühendislik Bilimleri Dergisi,* 31(1), 98-115, 2025.
[29] Teng ZJ, Lv J, Guo L. "An improved hybrid grey wolf optimization algorithm". *Soft computing*, 23, 6617-6631, 2019.